J. Quant. Spectrosc. Radiat. Transfer Vol. 35, No. 6, pp. 431–442, 1986
Printed in Great Britain.

0022–4073/86 $3.00 + .00
Pergamon Journals Ltd.

A RAPIDLY CONVERGENT ITERATIVE SOLUTION OF THE NON-LTE LINE RADIATION TRANSFER PROBLEM

GORDON L. OLSON and L. H. AUER
Los Alamos National Laboratory, Los Alamos, NM 87545, U.S.A.

and

J. ROBERT BUCHLER†
Physics Department, University of Florida, Gainesville, FL 32611, U.S.A.

(*Received* 21 *June* 1985; *Received for publication October* 1985)

Abstract—An iterative scheme has been developed for the solution of the non-LTE line radiation transfer problem. The method uses an approximate operator that is deliberately chosen to be local so that it can be easily extended to multidimensional geometry. The difference between the formal and approximate solutions is used as a driving term for the iterations. In one-dimensional, semi-infinite and free-standing slabs, the technique is found to be very fast, robust, and applicable to a large class of problems.

1. INTRODUCTION

While methods exist for the direct solution of the one-dimensional, non-LTE line-transfer problem (see the discussion by Mihalas[1] of the techniques by Feautrier[2] and Rybicki[3]), the development of a new general iterative technique for this problem is of great potential interest. The direct methods require the solution of large systems of linear equations; therefore, they are relatively expensive in both computer time and computer memory. The iterative method derived here uses an approximate operator that does not require the solution of any linear systems, not even banded systems. This can significantly reduce computer costs below those of the direct methods.

Iterative approaches are particularly advantageous when the radiation fields in a number of transitions must be found self-consistently. The equilivent two-level atom (ETLA) approach for multi-level atoms might then be used. A good guess for each radiation field is available from the previous ETLA cycle and can be used as a starting guess for the iterative solution in a given transition. In many problems the desired accuracy will only require a few iterations.

The difference between direct and iterative solutions is even greater in two dimensions. Direct solutions[4] and Monte Carlo simulations can be used; however, the computer requirements and computing costs are quite restrictive. Buchler and Auer[5] devised an iterative method that uses an operator which is a combination of an escape probability solution and a diffusion term. The result is a tridiagonal system of equations in one-dimensional problems; however, in two dimensions their operator introduces two nonzero diagonals far from the main diagonal. In the present paper we derive a local, i.e., diagonal, iterative technique for one-dimensional problems that remains diagonal when generalized to two-dimensional problems. The philosophy of Cannon[6,7] to use low order quadratures as approximate operators is here pushed to the limit of local operators. Preliminary results indicate that this approach also works well in two-dimensional slabs.

In the next section we define the problem of non-LTE line radiation transfer. Then in §3 we discuss iterative methods in terms of lambda iteration. Our new operator and its performance is presented in section 4. A method which works very well in accelerating the convergence of the iterations is given in §5 and our conclusions are in §6.

† Consultant at the Los Alamos National Laboratory.

2. DEFINITION OF THE PROBLEM

The class of radiation transfer problems which we are addressing are those in which the scattering term in the source function depends only on an integral of the radiation field over all directions and frequencies. Examples of such are the coherent scattering problem, the two-level non-LTE line transfer problem with complete redistribution, and the non-LTE continuum formation problem. For the sake of definiteness, we will present our technique as it applies to the non-LTE line problem.

We follow the notation of Mihalas[1] (Chapter XI). For simplicity, in the examples presented, we assume a uniform medium so that the thermal source term, B, the frequency integrated line opacity, χ, and the line profile, ϕ_x, which is normalized to have unit area, are all constant. Frequency is measured as the displacement from line center in Doppler units, x. In slab geometry, the spatial coordinate z is replaced by the optical depth τ defined by $d\tau = -\chi dz$.

In the case of a two-level atom without continuum, the source function is given by

$$S(\tau) = (1 - \epsilon)\,\bar{J}(\tau) + \epsilon B \quad , \tag{1}$$

with

$$\bar{J}(\tau) = \frac{1}{2}\int_{-\infty}^{+\infty} dx\ \phi_x \int_{-1}^{+1} d\mu\ I_x(\mu, \tau) \quad , \tag{2}$$

where ϵ is the thermalization parameter and μ is the cosine of the angle from the slab normal. The specific intensity, $I_x(\mu, \tau)$, is given by the solution of the radiation transfer equation:

$$\mu[\partial\, I_x(\mu, \tau)/\partial\tau] = \phi_x\,[I_x(\mu, \tau) - S(\tau)] \quad . \tag{3}$$

It is convenient to transform variables to the symmetric average of the specific intensity

$$u_x(\mu, \tau) \equiv [I_x(\mu, \tau) + I_x(-\mu, \tau)]/2 \quad . \tag{4}$$

Then Eq. (2) becomes

$$\bar{J}(\tau) = \int_{-\infty}^{+\infty} dx\ \phi_x \int_0^1 d\mu\ u_x(\mu, \tau) \tag{5}$$

and the radiation transfer equation, Eq. (3), can be rewritten as a second order differential equation (see Mihalas[1], Chap. VI), namely,

$$\partial^2 u_x(\mu, \tau)/\partial\,\tau_x^2 = u_x(\mu, \tau) - S(\tau) \quad , \tag{6}$$

where $d\tau_x \equiv -\chi\phi_x dz/\mu$. This differential equation can be put into numerical difference form using a simple 3-point scheme or using the more accurate Hermite scheme developed by Auer.[8] Such methods discretize the continuous variable $u(\tau)$ into a set of equations for u_i, $i = 1,2,...,N$, corresponding to the values of u at the N optical depth points, τ_i, in terms of the source function at those points, S_i. The variables μ and x are likewise discretized using quadrature points and weights appropriate for the evaluations in Eq. (2). For most of the examples presented in this paper, we have used the Hermite method to solve the transfer equation but other methods including those based on integral equations could have been used.

Given a source function, $S(\tau)$, Eq. (6) can be solved explicitly one frequency-angle point at a time. This will yield the $u_x(\mu, \tau)$ values to be substituted into Eq. (5) to determine the mean intensity. This procedure is called a *formal solution* and can be represented by

$$\bar{J}(\tau) = \Lambda\,[S(\tau)] \quad . \tag{7}$$

Although Λ is never assembled as a matrix operator when solving real problems, for the following sections it will be necessary to compute Λ as a matrix in order to analyze its properties.

The full solution of the non-LTE line transfer problem is formally reduced to the simultaneous solution of Eqs. (1) and (7), which can be expressed in the combined form

$$S(\tau) = (1 - \epsilon)\,\Lambda[S(\tau)] + \epsilon B \quad . \tag{8}$$

All the slabs analyzed in this paper will be characterized by their total optical depth, T, and the coarseness of the optical depth grid which is logarithmically spaced symmetrically about the slab midplane. We define the number of mesh points used per decade in optical depth as ξ. All angle integrals use 3 Gaussian quadrature points per quadrant and all frequency integrals use enough frequency points to reach a point in the line profile wing where the slab becomes optically thin.

3. AN ITERATIVE METHOD

A straightforward iteration (the so-called lambda iteration) is of the form

$$S^{n+1} = (1 - \epsilon)\Lambda[S^n] + \epsilon B \quad , \tag{9}$$

where S^n is the nth iterate. It has extremely slow convergence properties[1] for optically thick slabs. The object of this paper is to devise an alternative iteration technique.

Cannon[6,7] has proposed a general iteration procedure of the form

$$S^{n+1} = (1 - \epsilon)\Lambda^*[S^{n+1}] + (1 - \epsilon)(\Lambda - \Lambda^*)\,[S^n] + \epsilon B \quad , \tag{10}$$

involving an intermediate operator Λ^*, which he chose to be a Λ operator evaluated with fewer angle-frequency quadrature points. The difference between the formal Λ solution and the approximate Λ^* solution serves as a lagged driving term on the right hand side. The critical point about the Λ^* operator is that it is implicit and, therefore, mitigates the fundamental difficulty in classical lambda iteration, namely, the slow propagation of information through the grid. Clearly, Λ^* must be chosen carefully. The desirable properties for Λ^* are: (a) it is simple enough to be computed easily and cheaply, and (b) it results in a rapid and stable convergence to the correct answer.

Scharmer[9] has proposed variations on Cannon's approximate operator technique based on core saturation models.[10] His approach generates matrices that are almost upper triangular in one-dimensional problems. This produces a very good approximation to Λ which is relatively simple to use. The main disadvantage of Scharmer's method is the difficulty of generalizing it to multidimensions. Such a generalization would be much more difficult than extending the banded system proposed by Buchler and Auer[5] to multidimensions. We should note that other schemes[10,11] have been developed to get around the inefficiency of classical lambda iteration that use physical models such as the core saturation approximation.

A diagonal matrix is the only form that Λ^* may have and still guarantee simplicity in the structure of the implicit equations represented by Eq. (10). It is the purpose of this section to show that the choice of a diagonal operator is possible, easily computed, and yields an iterative method which converges fast enough to be useful. Equation (10) may be solved for the advanced value of the source function

$$S^{n+1} = [1 - (1 - \epsilon)\Lambda^*]^{-1}\,[(1 - \epsilon)(\Lambda - \Lambda^*)\cdot S^n + \epsilon B] \quad . \tag{11}$$

Since Λ^* will be diagonal, this will actually be a scalar divide and we will find it convenient to represent Λ^* as a depth dependent function $\Lambda^*(\tau)$. In order to analyze the iteration scheme, we rewrite Eq. (11) as

$$S^{n+1}(\tau) = \mathrm{A}\cdot S^n(\tau) + \epsilon B(\tau)/[1 - (1 - \epsilon)\Lambda^*(\tau)] \quad . \tag{12}$$

where

$$\mathbf{A} \equiv [1 - (1 - \epsilon)\Lambda^*]^{-1} (1 - \epsilon)(\Lambda - \Lambda^*) \quad . \tag{13}$$

The matrix, **A**, of Eq. (13) is the amplification matrix and its properties will determine the properties of this iteration scheme. The error vector for each iteration can be expressed in terms of the eigenvectors of **A** and asymptoticaly the error will vary as $(\lambda_{max})^n$, where λ_{max} is the eigenvalue of **A** with the largest magnitude. If λ_{max} is greater than unity, then the iterations will diverge. If all eigenvalues are less than unity, the iterations are guaranteed to converge to the correct answer. The smaller the value of λ_{max}, the faster the iteration will converge.

The case with $\Lambda^* \equiv 0$ reduces to the classical lambda iteration. The maximum eigenvalue in this case with a Doppler profile is

$$\lambda_{max} \approx (1 - \epsilon)\,(1 - T^{-1}) \quad . \tag{14}$$

Clearly, for thick, strongly scattering problems with $T \gg 1$ and $\epsilon \ll 1$, the value of λ_{max} is much too close to unity for convergence in a practical number of iterations. As we will show below, including even a simple implicit Λ^* operator in the iterative cycle reduces λ_{max} sufficiently to permit the general use of the iterative scheme given by Eq. (11).

The requirement that our operator be a diagonal matrix led us to analyze the simple local form

$$\Lambda^* = \Lambda^*(\tau)\mathbf{I} = [1 - \beta p(\tau)]\mathbf{I} \quad , \tag{15}$$

where **I** is the unit diagonal matrix. Here $p(\tau)$ is the probability of photon escape from optical depth τ and is given by the expression[1]

$$p(\tau) = \frac{1}{2}\int_{-\infty}^{+\infty} dx\ \phi_x \int_0^1 d\mu \{ \exp[-\phi_x \tau/\mu] + \exp[-\phi_x (T - \tau)/\mu] \} \quad , \tag{16}$$

where T is the total optical depth of the slab. Figure 1 shows the variation of $|\lambda_{max}|$ with β for a slab with $T = 20000$, $\epsilon = 10^{-6}$, Doppler line profiles, and three different mesh sizes. This figure shows that the maximum eigenvalue moves from one solution to another at the minimum value for λ_{max}. Unfortunately, this transition point is grid sensitive. With a course grid in optical depth, say 3 points per decade ($\xi = 3$), the minimum value of λ_{max} is smaller than if a fine grid is used. Thus iterations done with a course mesh can converge

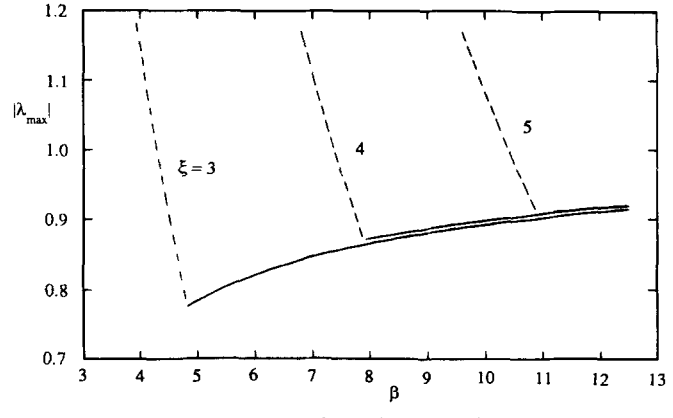

Fig. 1. The absolute value of the maximum eigenvalue, λ_{max}, is shown as a function of the β parameter in Eq. (15), for a slab with $T = 20000$, $\log(\epsilon) = -6$, and three values for the number of points per decade, ξ, as shown. The dashed lines are negative in value.

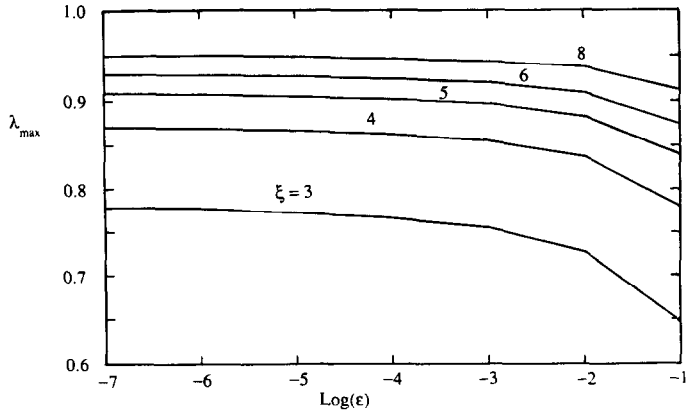

Fig. 2. The maximum eigenvalue is shown as a function of the destruction probability, ϵ, in a slab with Doppler profiles, $T = 20000$, $\beta = 3.111\xi - 4.447$ in Eq. (15), and 5 values for ξ.

faster, as well as being faster to compute. The value of β which gives the smallest λ_{max} is a linear function of ξ: $\beta = 3.111\xi - 4.447$.

Using the optimum value of β, Fig. 2 shows how λ_{max} depends on ϵ, the destruction probability. These values are all significantly smaller than Eq. (14) gives for classical Λ iterations. For small values of ϵ, the amplification matrix and λ_{max} become independent of ϵ. For large values of ϵ, the eigenvalues decrease as the problem becomes more tightly coupled to the thermal source B. This effect is partially a result of the $(1 - \epsilon)$ factor in the amplification matrix, Eq. (13). For very fine optical depth grids, the eigenvalues go asymptotically to 1.

4. A NEW ITERATIVE METHOD

The choice of Λ^* which yields the absolutely minimum value for λ_{max} is computationally formidable, but a set of values which is close to optimal is simply the diagonal of Λ. That this yields eigenvalues significantly smaller than unity can be shown by using Gerschgorin's theorem.[12] The theorem assures that if we subtract off the diagonal, then the largest eigenvalue is bounded by the sum of the off diagonal elements of the rows of the matrix. Since the elements of Λ should all be positive and the sum of any row is less than unity in magnitude, a little analysis will place limits on the value of λ_{max}.

The bound set by Gerschgorin's theorem can be stated in terms of the amplification matrix as

$$\lambda_{max} \leq \text{maximum}(\Sigma_j |A_{ij}|), \text{ for any } i \quad , \tag{17a}$$

or

$$\lambda_{max} \leq \text{maximum}\{ [1 - (1 - \epsilon)\Lambda^*(\tau_i)]^{-1} (1 - \epsilon) [\Sigma_j |\Lambda_{ij}| - \Lambda^*(\tau_i)] \} \quad . \tag{17b}$$

For convenience we define the vector $L(\tau)$ to be the result of a formal solution with the source function everywhere set to unity, i.e., $L(\tau) \equiv \Lambda[S(\tau) = 1]$. We can then replace the summation in Eq. (17b) by $L(\tau)$ and define

$$A(\tau) \equiv (1 - \epsilon)[L(\tau) - \Lambda^*(\tau)]/[1 - (1 - \epsilon)\Lambda^*(\tau)] \quad . \tag{18}$$

Then one can restate the limit on eigenvalues in terms of this depth dependent function as $\lambda_{max} \leq$ maximum of $A(\tau)$. If small optical depth steps are taken near the boundaries of thick slabs, for example at $\tau = 0$, then $\Lambda^*(0) \approx 0$, $L(0) \approx 0.5$, and $A(0) \approx (1 - \epsilon)/2$. Therefore, boundaries do not appear to give any difficulties in obtaining reasonable con-

vergence rates. At large depths, the Λ matrix becomes diagonally dominant and the upper limits on λ_{max} from these regions go to zero. Thus subtracting off the diagonal completely avoids the problem of propagation of information through thick layers which is so disastrous for the classical lambda iteration approach.

In practice, we do not want to explicitly calculate Λ in order to subtract its diagonal, because calculating Λ requires N formal solutions. Therefore, we need a quick and accurate method for estimating the diagonal of Λ. This can be done by examining the difference equation form for Eq. (6). The Hermite difference equation requires knowledge from three points: $u_{i-1}, u_i, u_{i+1}, S_{i-1}, S_i, S_{i+1}$. Rather than solving the tridiagonal system of equations in order to determine u_i (and all the other u), we found that a good approximation is to set

$$S_i = 1, S_{i\pm1} = 0 \quad , \tag{19a}$$

$$u^*_{i-1} = u^*_i \exp[-\phi_x(\tau_i - \tau_{i-1})/\mu] \quad , \tag{19b}$$

and

$$u^*_{i+1} = u^*_i \exp[-\phi_x(\tau_{i+1} - \tau_i)/\mu] \quad . \tag{19c}$$

With these substitutions into the difference equation form for Eq. (6), a local algebraic equation is obtained for u^*_i which can be inserted into

$$\Lambda^*_{ii} = \Lambda^*(\tau_i) = \int_{-\infty}^{+\infty} dx\, \phi_x \int_0^1 d\mu\, u^*_i \quad . \tag{20}$$

At the boundaries, substitutions similar to those of Eqs. (19) are made into the difference equations used for the boundary conditions. This calculation gives a good estimate of the ith diagonal element of Λ for the same computer cost as evaluating the escape probability in Eq. (16). This method for determining Λ^* is somewhat analogous to the escape probability formalism of Eqs. (15) and (16).

Figure 3 shows the maximum eigenvalues of the amplification matrix when Eq. (20) is used with Doppler line profiles. The eigenvalues for small ϵ are nearly identical to those in Fig. 2, while for large ϵ the eigenvalues are smaller and therefore better. Subtracting a deliberately chosen approximation to the matrix's diagonal is superior to parameterizing the escape probability function. The only trend not shown by Fig. 3 is that the eigenvalues decrease for thin slabs.

The big advantage of this result over that of the previous section is that good eigenvalues can be obtained without an adjustable parameter. Given the optical depth, angle, and frequency grids, Λ^* is calculated automatically to be consistent with the Λ operator.

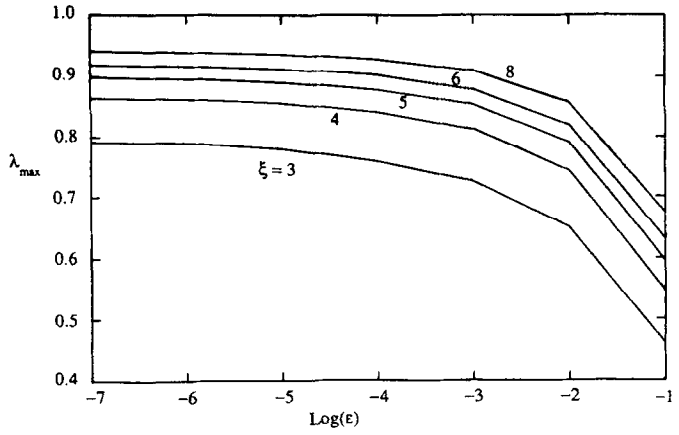

Fig. 3. As in Fig. 2, except that Eqs. (19) and (20) are used for Λ^*.

The dependence of λ_{max} on the coarseness of the spatial mesh can be intuitively understood in terms of communication along the computational grid rather than in physical optical depth space. In a pure Λ iteration, communication of the solution propagates on the order of one optical depth per iteration. Thus, problems with large thermalization depths require large numbers of iterations. Use of the Λ^* operator subtracts an analytic solution that mimics the true solution's value locally. Since Λ^* is moved to the left hand side of the equation, it is implicit in the solution for the next iteration values. Therefore, information is no longer limited to propagating on the optical depth scale, but is instead limited to propagating on the discrete grid. With a fine grid, the information must go through more points in order to propagate the same distance in optical depth; therefore, the eigenvalues are larger with a fine grid.

The usefulness of the technique does not depend on the type of line profile. For example, Lorentz profiles were used calculate the eigenvalues shown in Fig. 4. The general behavior is similar except that the eigenvalues for a Lorentz profile are smaller than for a Doppler profile and are bounded away from unity in the large ξ limit. Voigt profiles produce eigenvalues that are intermediate between Doppler and Lorentz.

For comparison, the results from a grey atmosphere (one frequency point) calculation are shown in Fig. 5. The grey case is relatively more difficult than the line transfer problem and, as shown in Fig. 5, eigenvalues are larger that in the Doppler case. The approximation to the diagonal of the Λ matrix, given by Eq. (20), has errors large enough for some values of ϵ and T to cause divergence of the iterations for the Hermite equations, even though Eq. (17) guarantees convergence if the true diagonal is used. The ordinary 3-point difference equations, which are second order accurate, are more strongly diagonally dominant and can be used in this iterative scheme through out the range of parameters shown in Fig. 5. The fact that the present technique solves the grey problem, which is pure coherent scattering, shows that it is not a disguised form of the core-wing approximation.

The differences in the values of the eigenvalues among the different profile shapes and the grey case are caused by the denominators of Eqs. (13) and (17). This factor goes to ϵ^{-1} at large optical depths, where Λ^* goes to unity. Therefore, the numerators must go accurately to zero. Just as the variation of the escape probability with optical depth changes significantly with different line profile shapes, so do $\Lambda^*(\tau)$ and $A(\tau)$. The variation of $A(\tau)$ with optical depth for the three cases is shown in Fig. 6. The peak values on the three curves are 0.994, 0.89, and 0.74, while the actual maximum eigenvalues are 0.91, 0.84, and 0.65, respectively. The location and width of the $A(\tau)$ function are related to the thermalization properties of the problem.

A very interesting feature of Fig. 6 is that the peaks where $A(\tau)$ is maximum shift in position only slightly as ϵ, T, ξ is varied. All slabs thicker than about 50 optical depths have nearly identical eigenvalues and convergence properties. A semi-infinite slab is not worse than a slab of 100 optical depths. Again, this is due to the fact that at large optical

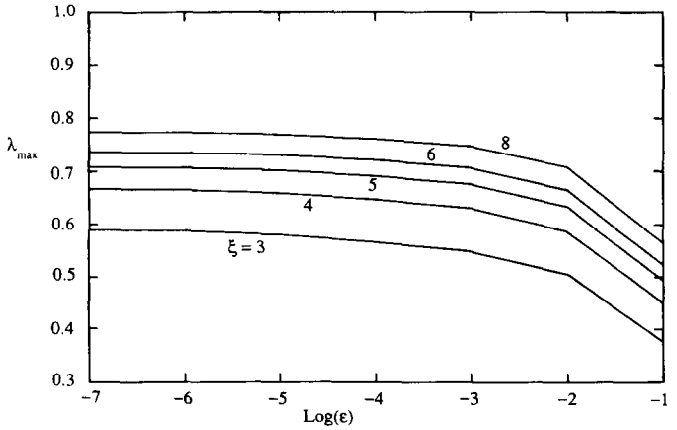

Fig. 4. As in Fig. 3, except that Lorentz profiles are used in a slab with $T = 2 \times 10^8$.

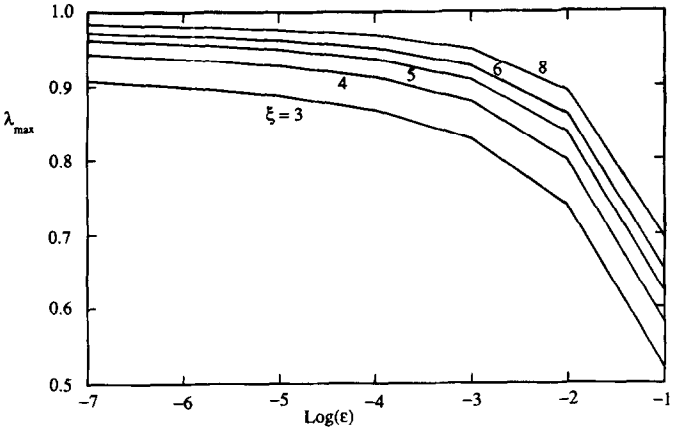

Fig. 5. As in Fig. 4, except that a grey opacity is used with simple 3-point differences.

depths the Λ matrix becomes nearly diagonal. Therefore, adopting a diagonal operator is an excellent approximation at large τ.

How does this iterative technique work in practice? Figure 7 shows the convergence of this iteration method for the case of $T = 2000$, $\epsilon = 0.001$, and $\xi = 4$. The convergence is stable and monotonic as is expected from our knowledge of λ_{max}. Unfortunately, this operator [Eq. (20)] provides an initial guess that is far from the final answer and this large value of λ_{max} causes the convergence to be somewhat slow. The latter problem will be addressed in the next section. The first problem can be reduced considerably by using a simple, first order escape probability solution to estimate the source function

$$S(\tau) = \epsilon B(\tau)/\{ 1 - (1 - \epsilon)[1 - p(\tau)]\} \quad . \tag{21}$$

Figure 8 shows the result when this modification of the method is applied to the same calculation as shown in Fig. 7. Now the initial guess is very good at large optical depth and only the surface layers are left to converge. The same case calculated with a Lorentz-profile would converge much faster.

If we were solving this radiation transfer problem as a coupled set of linear equations, this Λ^* iteration procedure would look exactly like Jacobi iteration. However, we are not solving this as a matrix problem. We never evaluate or use the full Λ matrix. In order to emphasize this fact, we can rewrite Eq. (12) as

$$[1 - (1 - \epsilon)\Lambda^*(\tau)] S^{n+1}(\tau) = (1 - \epsilon) [\bar{J}^n(\tau) - \bar{J}^{*n}(\tau)] + \epsilon B(\tau) \quad , \tag{22}$$

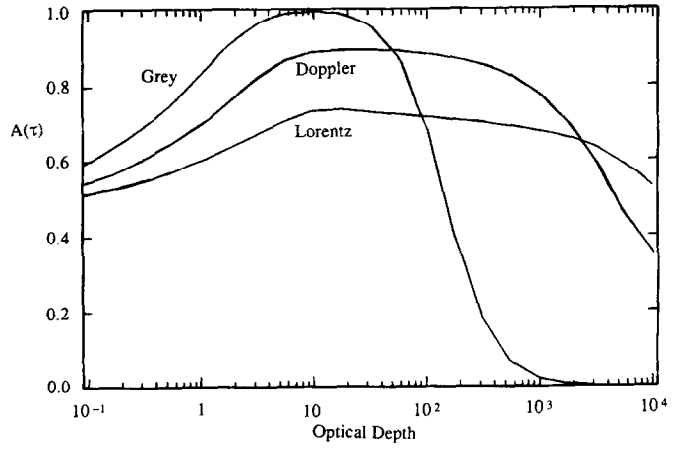

Fig. 6. The function $A(\tau)$ from Eq. (17) is shown for three cases.

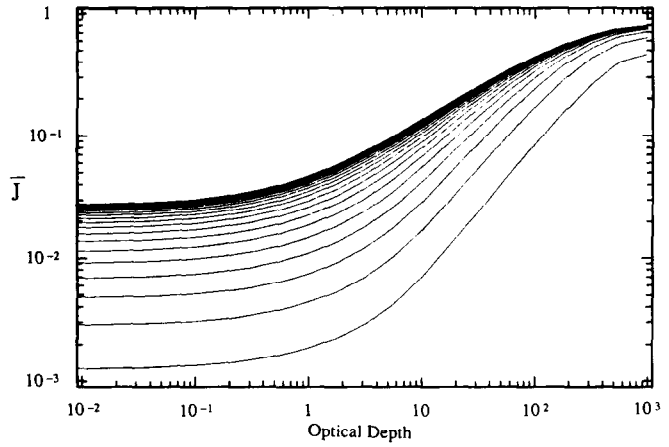

Fig. 7. The mean radiation field as a function of optical depth is shown for 20 iterations in half of a symmetric slab. The slab parameters are: Doppler profiles, $T = 2000$, $\epsilon = 0.001$, and $\xi = 4$.

where $\bar{J}^n(\tau)$ is the nth formal solution of Eqs. (5) and (6), and $\bar{J}^{*n}(\tau)$ is given by

$$\bar{J}^{*n}(\tau) = \Lambda^*(\tau)S^n(\tau) \quad . \tag{23}$$

After using Eq. (21) for an initial guess, both $\bar{J}^0$ and $\bar{J}^{*0}$ can be calculated. This procedure defines all terms on the right hand side of Eq. (22), and this equation can then be solved for $S^1(\tau)$. With this new source function, new J's can be calculated and the cycle repeated until convergence is obtained. The function $\Lambda^*(\tau)$ needs to be calculated only once, before the iteration cycle begins.

5. AN ACCELERATION METHOD

In order to improve the rate of convergence, Buchler and Auer[5] proposed the use of a very powerful acceleration method developed by Ng,[13] the three-point version of which we describe here. We consider an iteration of the form $\mathbf{x}^{n+1} = \mathbf{F}(\mathbf{x}^n)$. This is exactly the form of Eq. (22) where the vector $\mathbf{x}^n$ denotes $S^n(\tau)$ on the grid points.

We assume the iteration scheme is linearly convergent and we accelerate that convergence by adopting a linear combination of three successive iterations as follows:

$$\mathbf{x}^* = (1 - a - b)\mathbf{x}^{n-1} + a\,\mathbf{x}^{n-2} + b\,\mathbf{x}^{n-3} \tag{24}$$

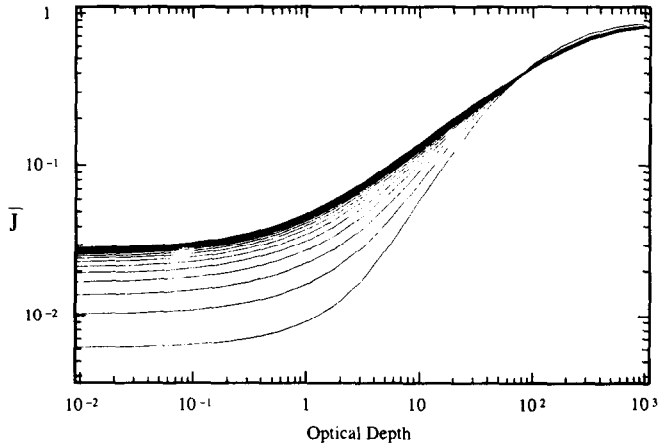

Fig. 8. As in Fig. 7, except that Eq. (21) is used for an initial guess.

and, thus,

$$\mathbf{F}(\mathbf{x}^*) = (1 - a - b)\mathbf{x}^n + a\,\mathbf{x}^{n-1} + b\,\mathbf{x}^{n-2} \quad . \tag{25}$$

The two unknown constants a and b are chosen to minimize the quantity

$$\Omega = \sum_{i=1}^{N} [x_i^* - F(x_i^*)]^2\, W_i \quad , \tag{26}$$

where W has been introduced as a weighting vector. This procedure takes a general vector and its next iteration's value, and minimizes the difference between them. The result is the linear set of equations

$$a\,A_1 + b\,B_1 = C_1 \quad , \tag{27a}$$

$$a\,A_2 + b\,B_2 = C_2 \quad , \tag{27b}$$

where

$$A_1 = \sum_{i=1}^{N} (x_i^n - 2x_i^{n-1} + x_i^{n-2})^2\, W_i \quad , \tag{28a}$$

$$B_1 = \sum_{i=1}^{N} (x_i^n - x_i^{n-1} - x_i^{n-2} + x_i^{n-3})\, W_i\, (x_i^n - 2x_i^{n-1} + x_i^{n-2}) \quad , \tag{28b}$$

$$A_2 = B_1 \quad , \tag{28c}$$

$$B_2 = \sum_{i=1}^{N} (x_i^n - x_i^{n-1} - x_i^{n-2} + x_i^{n-3})^2 W_i \quad , \tag{28d}$$

$$C_1 = \sum_{i=1}^{N} (x_i^n - 2x_i^{n-1} + x_i^{n-2})(x_i^n - x_i^{n-1}) W_i \quad , \tag{28e}$$

$$C_2 = \sum_{i=1}^{N} (x_i^n - x_i^{n-1} - x_i^{n-2} + x_i^{n-3})(x_i^n - x_i^{n-1}) W_i \quad , \tag{28f}$$

which can be readily be solved for

$$a = (C_1B_2 - C_2B_1)/(A_1B_2 - A_2B_1) \quad , \tag{29a}$$

$$b = (C_2A_1 - C_1A_2)/(A_1B_2 - A_2B_1) \quad . \tag{29b}$$

The iterate $\mathbf{x}^n$ is then replaced by the extrapolated value

$$\mathbf{x}^* = (1 - a - b)\mathbf{x}^n + a\,\mathbf{x}^{n-1} + b\,\mathbf{x}^{n-2} \quad , \tag{30}$$

which follows from Eq. (25). In principle, this accelerated vector can be calculated after the first four iterations, and after every following iteration. In practice, after the first acceleration, it was found desirable to calculate three new iterations before again using Ng's acceleration technique. Otherwise, this technique may not have enough independent information to form a good extrapolation to the solution.

The use of proper weighting is very important. In problems with small values for ϵ, $\bar{J}(\tau)$ will vary greatly and, unless properly weighted, regions of small $\bar{J}$ will not be adequately

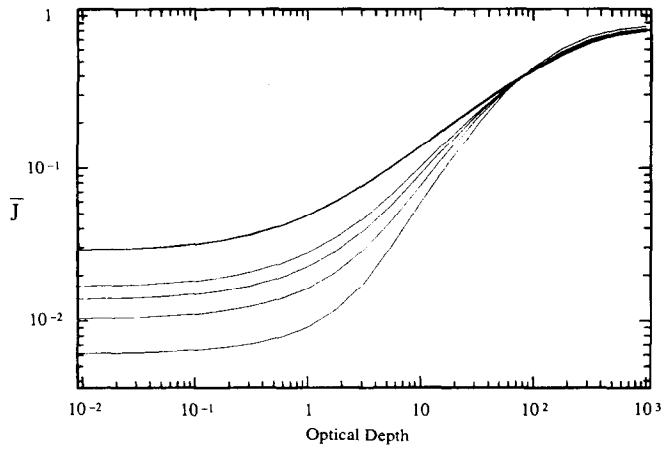

Fig. 9. As in Fig. 8, except that Ng's acceleration is used.

treated. We have found that the best weighting to use for transfer problems is $W(\tau_i) = [\bar{J}^n(\tau_i)]^{-1}$, where $\bar{J}^n$ is the current iteration value.

Figure 9 shows the application of this acceleration method to the problem presented in Fig. 8. After the initial four iterations, the accelerated solution jumps to within 2% of the final solution. This is a very typical example and shows that the combination of a relatively slow but stable iteration technique coupled with Ng's acceleration provides a robust method. The effective eigenvalue of this combination is near 0.4. For comparison, Scharmer's effective eigenvalue of 0.2 requires the solution of a matrix system much more complicated than our diagonal operator. The acceleration method presented here compensates for the simplicity of the diagonal Λ^*.

6. THE METHOD'S ROBUSTNESS AND CONCLUSIONS

In the region of parameter spaced spanned by $20 \leq T$, $-9 \leq \log(\epsilon) \leq -1$, and $3 \leq \xi \leq 10$, we have thoroughly studied the behavior of the maximum eigenvalue of the amplification matrix, λ_{max}, for Doppler and Lorentz profiles. At representative points, we have done the iterative solution of the line radiation transfer problem in order to confirm the convergence properties. The combination of using the Λ^* which approximates the diagonal of the Λ matrix [Eqs. (19) and (20)] and Ng's acceleration worked well in all cases.

Linear or quadratic variations of the thermalization parameter, ϵ, with optical depth change λ_{max} only slightly. The important values of ϵ are those near the maximum of $A(\tau)$.

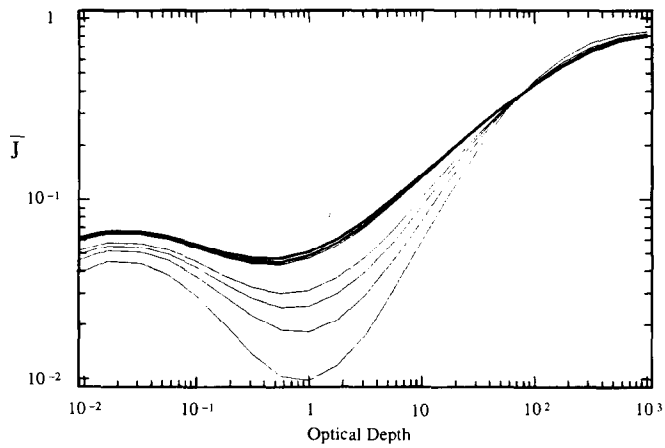

Fig. 10. As in Fig. 9, except that the velocity specified by Eq. (31) is used.

Variations in the thermal source, B, do not enter into the amplification matrix and thus can not affect the eigenvalues or the convergence properties.

Complications to the radiative transfer problem, such as variable line profiles or velocity fields, can be treated in the same way as presented here. As long as the numerical difference equations used to solve the problem are an adequate representation of the formal solution, approximations such as in Eq. (19) can be used to calculate an estimate to the diagonal of the Λ matrix. For example, Fig. 10 shows a calculation with a symmetric non-monotonic velocity field given by

$$v(t) = -2 \sin(\log_{10} t)/(1 + t^{1/2}) \quad , \tag{31}$$

where t = minimum $(\tau, T - \tau)$. This velocity law is similar to one presented by Scharmer.[9]

The one possible problem with this iterative technique might be its grid sensitivity. It is not always possible to choose the optimum grid for every line transfer problem. Therefore, we experimented with using different mesh refinements in different parts of a problem. We concluded that the important region is from optical depth 1 to the thermalization depth, just as one could predict from looking at the plots of $A(\tau)$ shown in Fig. 6. The structure of the grid at the surface or deep inside the slab had no effect on λ_{max}. The technique has been analyzed here with a logarithmically spaced symmetric grid in order to simplify the analysis, but the technique is not limited to this grid structure. The finest grid structure in the first thermalization depth determines the largest eigenvalue.

Because of its simplicity and robustness, the technique developed in this paper looks very attractive. In terms of computer codes, this method with only formal solutions to evaluate is much simpler than solving the problem with either the Feautrier[2] or Rybicki[3] technique. Its purely local nature gives it a diagonal matrix representation that is still diagonal in multidimensional geometry. Therefore, this simplicity is retained in higher dimensions. Preliminary results show that the iterative technique works as well in two dimensions as it does in one.

REFERENCES

1. D. Mihalas, *Stellar Atmospheres*, Freeman & Co., San Francisco (1978).
2. P. Feautrier, *C. R. Acad. Sci. Paris* **258**, 3189 (1964).
3. G. B. Rybicki, *JQSRT* **11**, 589 (1971).
4. D. Mihalas, L. H. Auer, and B. R. Mihalas, *Ap. J.* **220**, 1001 (1978).
5. J. R. Buchler and L. H. Auer, in *Proceedings of the 2nd International Conference and Workshop on the Radiative Properties of Hot Dense Matter*, (Sarasota, 31 Oct 1983), ed. J. Davis, et al., World Scientific, Singapore (1985).
6. C. J. Cannon, *Ap. J.* **185**, 621 (1973).
7. C. J. Cannon, *JQSRT* **13**, 627 (1973).
8. L. H. Auer, *JQSRT* **16**, 931 (1976).
9. G. B. Scharmer, in *Methods in Radiative Transfer*, ed. W. Kalkofen, Cambridge University Press, London, UK (1984).
10. G. B. Rybicki, "*Conference on Line Formation in the Presence of Magnetic Fields*," National Center for Atmospheric Research, Boulder, CO, unpublished (1971).
11. J. P. Apruzese, J. Davis, D. Duston, and R. W. Clark, *Phys. Rev. A.* **29**, 246 (1984).
12. J. H. Wilkinson, *The Algebraic Eigenvalue Problem*, Clarendon Press, Oxford, UK (1965).
13. K. C. Ng, *J. Chem. Phys.* **61**, 2680 (1974).